Bulletin of the Seismological Society of America, Vol. 81, No. 6, pp. 2186–2193, December 1991

A PRELIMINARY DESCRIPTIVE MODEL FOR THE DISTANCE DEPENDENCE OF THE SPECTRAL DECAY PARAMETER IN SOUTHERN CALIFORNIA

BY JOHN G. ANDERSON

ABSTRACT

The spectral decay parameter, κ, defined by Anderson and Hough (1984) is described as a function of distance, R, and site, S, as $\kappa(R,S) = \kappa_0(S) + \tilde{\kappa}(R)$. The terms $\tilde{\kappa}(R)$ and $\kappa_0(S)$ are found by a method that is unbiased by prior assumptions about the nature of the distance dependence. Variance using this model is substantially smaller than in simpler models that do not incorporate both site effects and a distance effect. For data gathered near Anza, California, and for distances less than 100 km, $\tilde{\kappa}(R)$ is very similar for both P- and S-wave windows, but $\kappa_0(S)$ is smaller for P than for S on average by a factor of about 2.

INTRODUCTION

The spectral decay parameter, κ, is an observational parameter of the spectrum of earthquake ground motion. The basic observation (Anderson and Hough, 1984) is that, at high frequencies, the spectrum of ground acceleration falls off exponentially with frequency, f, i.e.,

$$A(f) \propto A_0 \exp(-\pi\kappa f). \tag{1}$$

In its action on the seismic spectrum, κ may be compared with t^*, but is only equal to t^* under specialized assumptions (e.g., Hough *et al.*, 1988).

The basic characteristics of the spectral decay parameter in California, as described by Anderson and Hough (1984), Anderson (1986), and Hough *et al.* (1988) are that (1) for a single site, κ has a slight, but meaningful, increase as the epicentral distance increases and (2) the curve $\kappa(R)$ moves upward or downward as a whole from site to site. A clear illustration of these observations is presented in Anderson (1986) and Hough *et al.* (1988), where $\kappa(R,S)$ follows approximately parallel trends for stations in Imperial Valley, on deep sediments, and at Piñon Flat Observatory, on granite with a thin weathered layer. The numerical values of κ at Piñon Flat are about 0.06 sec smaller than in Imperial Valley at all distances.

A mathematical formulation of this is to regard $\kappa(R,S)$ as a function of epicentral distance, R, and a categorical variable to identify the site, called S here, as follows:

$$\kappa(R,S) = \kappa_0(S) + \tilde{\kappa}(R), \tag{2}$$

where $\kappa_0(S)$ takes a unique value for each site. The distance dependence is entirely described by $\tilde{\kappa}(R)$, which is constrained to equal zero at zero distance.

There are several practical motivations for obtaining a description of $\tilde{\kappa}(R)$. First, such a description will facilitate comparisons among regions, where $\tilde{\kappa}(R)$ might differ. Second, it may be interesting to know $\kappa_0(S)$ for a new site (for earthquake engineering or geophysical investigations) and a reliable $\tilde{\kappa}(R)$

curve will allow $\kappa_0(S)$ to be estimated from a few earthquakes at arbitrary distances. Third, if κ is an attenuation parameter and $\tilde{\kappa}(R)$ is controlled by the Q profile, as a function of depth, then a better model of $\tilde{\kappa}(R)$ would allow a better estimation of Q. Furthermore, to the extent that the exponential decay describes the shapes of spectra at high frequencies, a good model for $\tilde{\kappa}(R)$ will allow applications in generation of synthetic seismograms by stochastic (e.g., Boore, 1983) and other procedures. Finally, a standard model of κ allows recognition of anomalous values, which might serve to indicate anomalous sources or anomalous attenuation, such as from crossing fault zones.

METHOD FOR FITTING $\tilde{\kappa}(R)$

As a first approximation, Anderson and Hough (1984) and Hough *et al.* (1988) fit $\tilde{\kappa}(R)$ by a linear regression. However, there is no basis for assuming any particular distance dependence. Thus the only constraint that this paper imposes is that $\tilde{\kappa}(R)$ is a smooth function of R. The intent is similar to that of the nonparametric regression for peak acceleration developed by Brillinger and Preisler (1984). The numerical method is similar to the one used by Castro *et al.* (1990), with three differences. Castro *et al.* (1990) described spectral amplitudes with a nonparametric distance dependence and a categorical variable giving the zero-distance amplitude of each earthquake. In the present case, the categorical variable is $\kappa_0(S)$. Second, in this case, data at distances between the discertized points where $\tilde{\kappa}(R)$ is actually evaluated are treated differently; a linear interpolation between the discretized points is used. Finally, the smoothness criteria limit changes in the third derivative of $\tilde{\kappa}(R)$ instead of the second derivative as in Castro *et al.* (1990). The results below are insensitive to deletion of half the data at random for distances less than 200 km, suggesting that $\tilde{\kappa}(R)$ is stable with respect to data input.

NUMERICAL RESULTS

For data, this paper uses observations of κ for both P and S waves, determined by Hough (1987) and Hough *et al.* (1988), from 10 digital seismic stations in the Anza network in southern California. It also uses S-wave observations from Anderson and Hough (1984) for the Imperial Valley. Maps of events and stations are found in Hough *et al.* (1988) and Anderson and Hough (1984).

Table 1 lists $\tilde{\kappa}(R)$ for P and S waves, and Figures 1 and 2 show the fit of these curves to the data for each station. Table 2 lists $\kappa_0(S)$ for every station. Finally Figure 3 compares $\tilde{\kappa}(R)$ derived for P and S waves. Figures 1 and 2 demonstrate that the data match the trend of the average curve without exception. Table 1 also lists the number of data in each distance range which contribute to the determination of $\tilde{\kappa}(R)$. Six S-wave data and 11 P-wave data at distances beyond 200 km further constrain the results. The number of data drop off quickly for distances beyond 100 km, implying that the numerical estimates for $\tilde{\kappa}(R)$ beyond 100 km are less reliable than at shorter distances. The model is truncated at 200 km because the number of data beyond 200 km is very small and the smoothness constraints influence the fit to the data there.

The model in Figures 1 and 2 is a rather complex description for the parameter κ. Using analysis of variance (Mason *et al.*, 1989), it can be shown that the model given in Tables 1 and 2 for both P and S waves is statistically better than each of the following, given in order of increasing numbers of

TABLE 1

PRELIMINARY NUMERICAL VALUES FOR $\tilde{\kappa}(R)$ IN SOUTHERN CALIFORNIA

	S Waves		P Waves	
R (km)	$\tilde{\kappa}(R)$* (msec)	# data†	$\tilde{\kappa}(R)$* (msec)	# data†
0	0.0	13	0.0	20
10	3.5	57	2.7	28
20	5.7	62	4.8	32
30	6.9	51	6.3	27
40	6.9	40	7.7	18
50	6.5	80	9.6	29
60	7.9	70	12.4	23
70	11.1	58	16.1	26
80	15.5	36	19.5	12
90	21.9	52	21.9	26
100	28.7	22	23.7	6
110	34.0	8	25.6	7
120	37.3	10	27.5	6
130	39.1	9	29.0	3
140	40.6	3	29.8	3
150	42.5	8	29.9	3
160	44.3	2	29.6	2
170	45.5	4	29.4	2
180	46.4	4	29.0	1
190	48.5	6	28.2	3
200	53.3	0	27.0	1

$\tilde{\kappa}(R)$ is determined using a linear interpolation between points.

†This is the number of values of kappa that are available at a distance that rounds off to the corresponding distance in the table.

unknown parameters:

Model 1: $\kappa(R, S) = constant$.

Model 2: $\kappa(R, S) = \kappa_0 + mR$.

Model 3: $\tilde{\kappa}(R) = 0$ and $\kappa_0(S)$ developed for each station.

Model 4: $\tilde{\kappa}(R) = mR$ and $\kappa_0(S)$ developed for each station.

In the context of the adopted fitting procedure, it would be easy to develop additional models with complexity intermediate between model 4 and the model given in Tables 1 and 2. This would be done by increasing the separation with distance, ΔR, between points at which $\tilde{\kappa}(R)$ is determined, until one finds the least complex distance dependence that is demanded by the data. The given model, with $\Delta R = 10$ km, probably has more parameters than necessary. However, even though large values for ΔR (e.g., 50 km) might be justified from a strictly numerical point of view, there is no physical justification for imposing a model in which changes in slope of $\tilde{\kappa}(R)$ occur only at large distance intervals. Thus, these models are not investigated. The procedural improvement of avoiding such unjustified artifacts in $\tilde{\kappa}(R)$ warrants the additional complexity in the preferred models. The RMS misfit in the preferred model is nearly a factor of 2 greater than an estimate for the standard deviation in

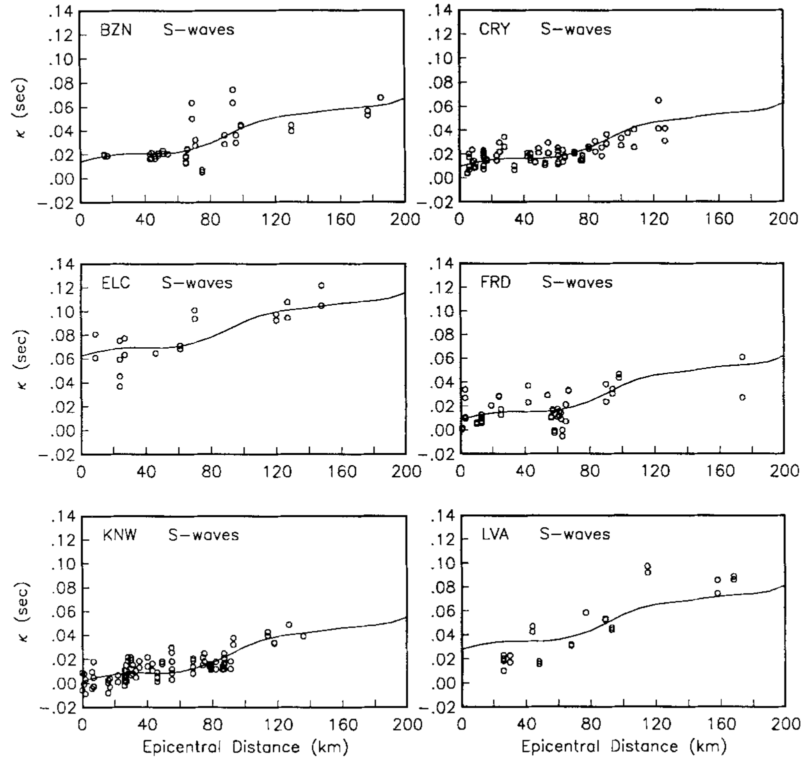

(a)

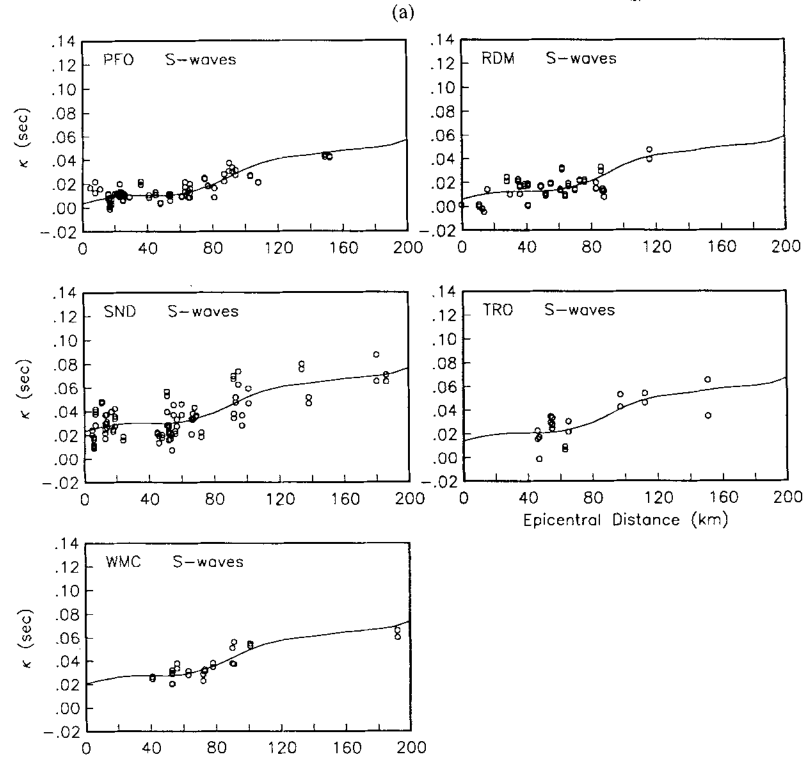

(b)

FIG. 1. Data and model $\kappa(R, S)$ for each station for S waves.

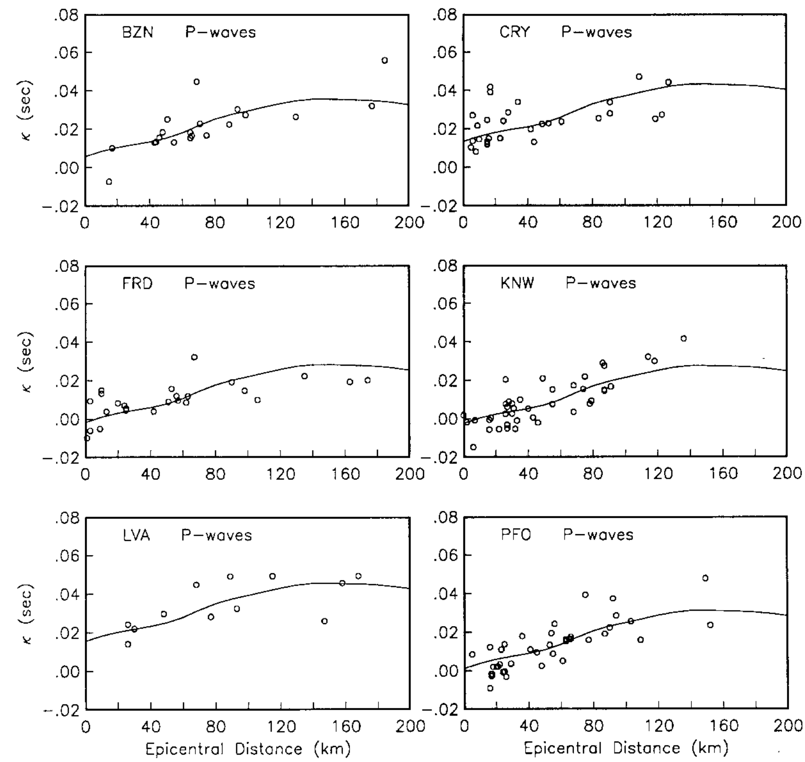

(a)

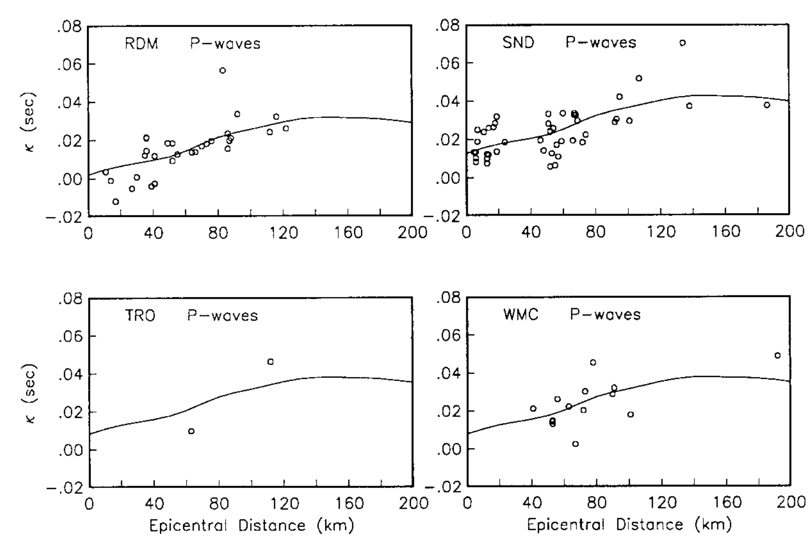

(b)

FIG. 2. Data and model $\kappa(R, S)$ for each station for P waves.

TABLE 2

PREFERRED ESTIMATES OF $\kappa_0(S)$ FOR THE STATIONS USED IN THIS STUDY

		S Waves		P Waves		Ratios	
Station	Geology*	$\kappa_0(S)$ (msec)	# data	$\kappa_0(S)$ (msec)	# data	$R_a^{\dagger}$	$R_b^{\ddagger}$
BZN	Decomposed tonalite Sloping terrain	13.8	43	5.6	22	2.5	1.4
CRY	Tonalite outcrop Nearly flat terrain	9.4	86	13.4	31	0.7	0.4
ELC	Deep alluvium Flat terrain	62.4	20				
FRD	Tonalite Near edge of shallow alluvial valley	8.5	47	−1.7	27	?	
KNW	Tonalite weathered to 20 m Small, low ridge on sloping terrain	1.9	96	−2.4	44	?	
LVA	Granodiorite Side of alluvial valley	27.9	26	15.5	13	1.8	1.1
PFO	Quartz diorite-granodiorite weathered to 20 m Flat terrain	3.6	88	1.2	40	3.0	1.7
RDM	Metamorphic pendant-gneiss Mt. peak	5.9	55	1.9	31	3.1	1.8
SND	Decomposed tonalite in San Jacinto fault zone	23.3	94	12.7	50	1.8	1.1
TRO	Quartz diorite-granodiorite outcrop Mt. peak	14.1	20	8.2	2	1.7	1.0
WMC	Alluvium estimated 60 m thick Gently sloping terrain	20.6	26	7.9	14	2.6	1.5

*Geology is summarized from Vernon (1989).

† $R_a = \left\{ \dfrac{\kappa_0(S) \textit{ for S waves}}{\kappa_0(S) \textit{ for P waves}} \right\}$

‡ $R_b = \dfrac{R_a}{1.7}$, and thus for a Poisson's ratio of 0.25, $R_b = \dfrac{Q_{Pi}}{Q_{Si}}$, where Q_{Pi} is the frequency independent contribution to attenuation of P waves, and Q_{Si} is the frequency independent contribution to attenuation of S waves.

individual elements of κ, implying that the present model is still an incomplete description of the spectral decay at high frequencies. It is likely that differences in source spectral shapes and laterally heterogeneous attenuation contribute significantly to the residual scatter.

Figure 3 shows that $\tilde{\kappa}(R)$ for P and S waves are similar to distances of 100 km but diverge beyond that point. Considering the small amount of data beyond 100 km, this feature should not be considered to be confidently resolved. The similarity of the estimates at distances less than 100 km is a significant feature and implies $Q_S > Q_P$ at the depth of seismic wave propagation, as found by Hough and Anderson (1988).

In Table 2, we observe a qualitative, although imperfect, relationship between $\kappa_0(S)$ and the site conditions. The two stations that are most nearly connected to unweathered plutonic rock, PFO and KNW, have the smallest values of $\kappa_0(S)$. ELC on deep Imperial Valley alluvium has the greatest value of $\kappa_0(S)$. Two other stations on alluvium or decomposed granitic rocks, SND and WMC, also have relatively high values of $\kappa_0(S)$. Anderson and Hough (1984), Anderson (1986), Hough *et al.* (1988), Hough and Anderson (1988) have

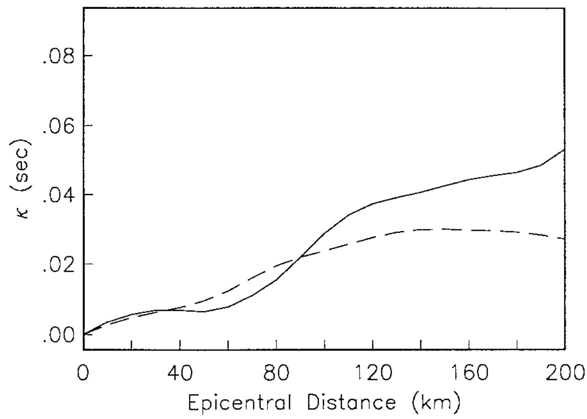

FIG. 3. $\tilde{\kappa}(R)$ for S (——) and P (- - -) data.

previously attributed $\kappa_0(S)$ to attenuation below the stations, and these results support that hypothesis qualitatively. For KNW and PFO, Fletcher *et al.* (1990) characterized the attenuation in the upper 130 m with values for t^* equal to 4 and 3 msec, respectively, agreeing within uncertainties with the present estimates of $\kappa_0(S)$ of 1.9 and 3.6 msec. Under the assumptions that cause t^* and κ to be the same (source spectrum has an ω^{-2} asymptote at high frequencies, a frequency-independent contribution to Q is separable, wave propagation and site resonances are small), this limited comparison is consistent quantitatively with the hypothesis that $\kappa_0(S)$ is caused by attenuation below the site.

Unlike the terms in $\tilde{\kappa}(R)$ for P and S waves, the station terms are not similar. Rather $\kappa_0(S)$ is smaller for P waves than for S waves at all but one station (CRY). Two stations yielded $\kappa_0(S)$ for P waves slightly less than zero, a result that can be attributed to small numerical values and observational uncertainty but might also result from a smaller than average increase in κ for distant earthquakes recorded at those stations. The ratio of $\kappa_0(S)$ for S to P waves from the other eight stations is 2.2 ± 0.8. As observed by Hough and Anderson (1988), this implies that Q_P is greater than Q_S, on the average, in the weathered layer.

DISCUSSION AND CONCLUSIONS

It would be reasonable to repeat the modeling of this paper with more estimates of κ, particularly for distances beyond 100 km. This would increase the confidence in the curves of $\tilde{\kappa}(R)$. However, since they are unaffected by removal of half the data at distances less than 200 km, it is not obvious that a substantial increase in the number of estimates of κ in the distances between 100 and 200 km will result in curves with a significantly different character. Our model (equation 2) has not included any attempt to observe variations with earthquake size (suggested by Hanks, 1982), and evaluation of this effect will need to wait for additional data sets.

Hough and Anderson (1988) modeled the distance dependence of κ to obtain a model for the depth dependence of Q. The results of this paper in contrast are only a description of the distance and site dependence of κ. However, the present curves might be used for several purposes, including comparison of

$\tilde{\kappa}(R)$ with other regions, estimating $\kappa_0(S)$ from earthquakes at arbitrary distances, constraining the shapes of spectra in synthetic seismograms, and studying the depth dependence of the frequency-independent contribution to Q. Finally, the model can be used as a starting point to better understand the remaining scatter in the data, since the RMS residual in the final model is still nearly twice the uncertainty in the data, implying that unmodeled signal remains.

Acknowledgments

The author thanks Sue Hough for supplying the data used in this study and for reviewing the manuscript. D. Boore, W. Peppin, and an anonymous reviewer suggested several improvements to the manuscript. The National Science Foundation research grant EAR 85 18647 supported the work done in this study.

References

Anderson, J. G. (1986). Implication of attenuation for studies of the earthquake source, in *Earthquake Source Mechanics, Maurice Ewing Series 6*, S. Das, J. Boatwright, and C. H. Scholz (Editors), American Geophysical Union, Washington, D.C., 311-318.

Anderson, J. G. and S. E. Hough (1984). A model for the shape of the Fourier amplitude spectrum of acceleration at high frequencies, Bull. Seism. Soc. Am. 74, 1969-1993.

Boore, D. M. (1983). Stochastic simulation of high frequency ground motions based on seismological models of the radiated spectra, *Bull. Seism. Soc. Am.* **73**, 1865-1894.

Brillinger, D. R. and H. K. Preisler (1984). An exploratory analysis of the Joyner-Boore attenuation data, *Bull. Seism. Soc. Am.* **74**, 1441-1450.

Castro, R. R., J. G. Anderson, and S. K. Singh (1990). Site response, attenuation and source spectra of S waves along the Guerrero, Mexico, subduction zone, *Bull. Seism. Soc. Am.* **80**, 1481-1503.

Fletcher, J. B., T. Fumal, H.-P. Liu, and L. C. Carroll (1990). Near-surface velocities and attenuation at two boreholes near Anza, California from logging data, *Bull. Seism. Soc. Am.* **80**, 807-831.

Hanks, T. C. (1982). f_{max}, *Bull. Seism. Soc. Am.* **72**, 1867-1879.

Hough, S. E. (1987). The attenuation of high frequency seismic waves, *Ph.D. Thesis*, University of California, San Diego, 157 pp.

Hough, S. E. and J. G. Anderson (1988). High-frequency spectra observed at Anza, California: Implications of Q structure, *Bull. Seism. Soc. Am.* **78**, 692-707.

Hough, S. E., J. G. Anderson, J. Brune, F. Vernon III, J. Berger, J. Fletcher, L. Haar, T. Hanks, and L. Baker (1988). Attenuation near Anza, California, *Bull. Seism. Soc. Am.* **78**, 672-691.

Mason, R. L., R. F. Gunst, and J. L. Hess (1989). Statistical design and analysis of experiments, Wiley, New York, 692 pp.

Vernon, F. L. (1989). Analysis of data recorded on the ANZA seismic network, *Ph.D. Thesis*, University of California, San Diego.

Seismological Laboratory and
Department of Geological Sciences
Mackay School of Mines
University of Nevada
Reno, Nevada 89557

Manuscript received 1 February 1991